The Structural Basis of Elasticity in Fibrillin-Based Microfibrils

ARTICLE *in* STRUCTURE · JUNE 2004

Impact Factor: 5.62 · DOI: 10.1016/j.str.2004.04.005 · Source: PubMed

1 AUTHOR:

M. Amin A Arnaout
Harvard Medical School
156 PUBLICATIONS **13,767** CITATIONS

preparation of carotenoid-reconstituted bRC samples which involves an obligatory sonication step. Roszak and coworkers point out that the treatment results in isomerization of about one-third of the all-*trans* spheroidene to a mixture of *cis* isomers. The agitation provided from sonication may also in some way facilitate carotenoid binding by opening the binding pocket for easier access of the carotenoid. It is interesting to note that even carotenoids locked into the *cis* conformation by a 6-membered ring at the position of the 15-15′-*cis* bond are capable of being incorporated into the carotenoid binding site (Bautista et al., 1998).

The architecture of the carotenoid binding pocket in the absence of the carotenoid indirectly reveals some details of how the molecule binds to the protein. A molecule of N,N-dimethyldodecylamine-N-oxide (LDAO), the detergent used to solubilize bRCs, is found in the carotenoid binding site in the absence of a carotenoid. With LDAO in the site, the phytyl tail of $BChl_B$, which is normally in contact with the carotenoid, shifts position and reduces the binding pocket size. The protein surrounding the carotenoid binding site retains nearly all of its geometry in the absence of the carotenoid, with the exception of the side chains of a few amino acids. In particular, a phenylalanine residue (Phe M162) rotates to occupy a portion of the carotenoid binding site. Roszak et al. (2004) explain that the motion of this amino acid restricts entry of the carotenoid to only one of the two solvent-exposed openings. The carotenoid presumably binds tail first in order to push past the phenylalanine, and the last portion of the carotenoid to enter the protein, the methoxy head group, is locked into place with a hydrogen bond. The gating action of this phenylalanine acts to admit the cofactor in the correct orientation. Roszak et al. (2004) in suggesting a plausible mechanism for binding the carotenoid to the protein in the correct orientation, open the way to further study of triplet state quenching by carotenoids in the bRC.

Cara A. Tracewell
Department of Chemistry
Yale University
P.O. Box 208107
New Haven, Connecticut 06520

Selected Reading

Agalidis, I., Lutz, M., and Reisshusson, F. (1980). Biochim. Biophys. Acta *589*, 264–274.

Arnoux, B., Ducruix, A., Reisshusson, F., Lutz, M., Norris, J., Schiffer, M., and Chang, C.H. (1989). FEBS Lett. *258*, 47–50.

Bautista, J.A., Chynwat, V., Cua, A., Jansen, F.J., Lugtenburg, J., Gosztola, D., Wasielewski, M.R., and Frank, H.A. (1998). Photosynth. Res. *55*, 49–65.

Boucher, F., Vanderrest, M., and Gingras, G. (1977). Biochim. Biophys. Acta *461*, 339–357.

Deisenhofer, J., Epp, O., Miki, K., Huber, R., and Michel, H. (1985). Nature *318*, 618–624.

Farhoosh, R., Chynwat, V., Gebhard, R., Lugtenburg, J., and Frank, H.A. (1997). J. Photochem. Photobiol. *66*, 97–104.

Frank, H.A., Chynwat, V., Posteraro, A., Hartwich, G., Simonin, I., and Scheer, H. (1996). Photochem. Photobiol. *64*, 823–831.

Frank, H.A., Desamero, R.Z.B., Chynwat, V., Gebhard, R., vanderHoef, I., Jansen, F.J., Lugtenburg, J., Gosztola, D., and Wasielewski, M.R. (1997). J. Phys. Chem A *101*, 149–157.

Krinsky, N. (1971). In Carotenoids, O. Isler, G. Guttman, and U. Solms, eds. (Basel, Switzerland: Birkhauser Verlag), pp. 669–716.

Lutz, M., Kleo, J., and Reiss-Husson, F. (1976). Biochem. Biophys. Res. Commun. *69*, 711–717.

Roszak, A.W., McKendrick, K., Gardiner, A.T., Mitchell, I.A., Isaacs, N.W., Cogdell, R.J., Hashimoto, H., and Frank, H.A. (2004). Structure *12*, this issue, 765–773.

Yeates, T.O., Komiya, H., Chirino, A., Rees, D.C., Allen, J.P., and Feher, G. (1988). Proc. Natl. Acad. Sci. USA *85*, 7993–7997.

Structure, Vol. 12, May, 2004, DOI 10.1016/j.str.2004.04.005

The Structural Basis of Elasticity in Fibrillin-Based Microfibrils

The resiliency of vertebrate tissues such as skin and blood vessels is generated by the elastic fiber network. A recent article by Lee and colleagues (Lee et al., 2004) provides intriguing new cues into the organization and structure of this network.

Elastic fibers are major components of the extracellular matrix (ECM) of vertebrate tissues such as skin, lung, and blood vessels that endow such tissues with the resilience needed for recoil when stretched. The main component of elastic fibers is elastin that is ensheathed by 10 nm fibrillin-rich microfibrils, which provide the template for the deposition and assembly of secreted tropoelastin monomers into insoluble elastic fibers (Zhang et al., 1995). In tissues lacking elastin (such as the zonular fibers of the eye), microfibrils provide the elasticity and resilience needed for lens accommodation. Inherited defects in fibrillin-1 in humans cause Marfans syndrome (Robinson and Godfrey, 2000), manifested by severe cardiovascular, skeletal, and ocular abnormalities, reflecting the critical contribution of fibrillins to tissue integrity.

Fibrillin-1, the major fibrillin of adult tissues, is a modular glycoprotein formed primarily of 43 rigid calcium binding EGF (cbEGF) domains, interspersed among which are seven "TB" (TGFβ binding-protein-like) modules. Isolated microfibrils have a characteristic bead on a string appearance, with an untensioned bead periodicity of 56 nm in the presence of bound calcium (Sherratt et al., 2003), indicating that the ~150 nm long fibrillin-1 molecule is highly folded within the microfibril (Baldock et al., 2001). Despite extensive studies, the precise molecular packing of fibrillin-rich microfibrils and therefore the basis of their elasticity remain unknown. A recent "jack-knife" model based on automated electron tomog-

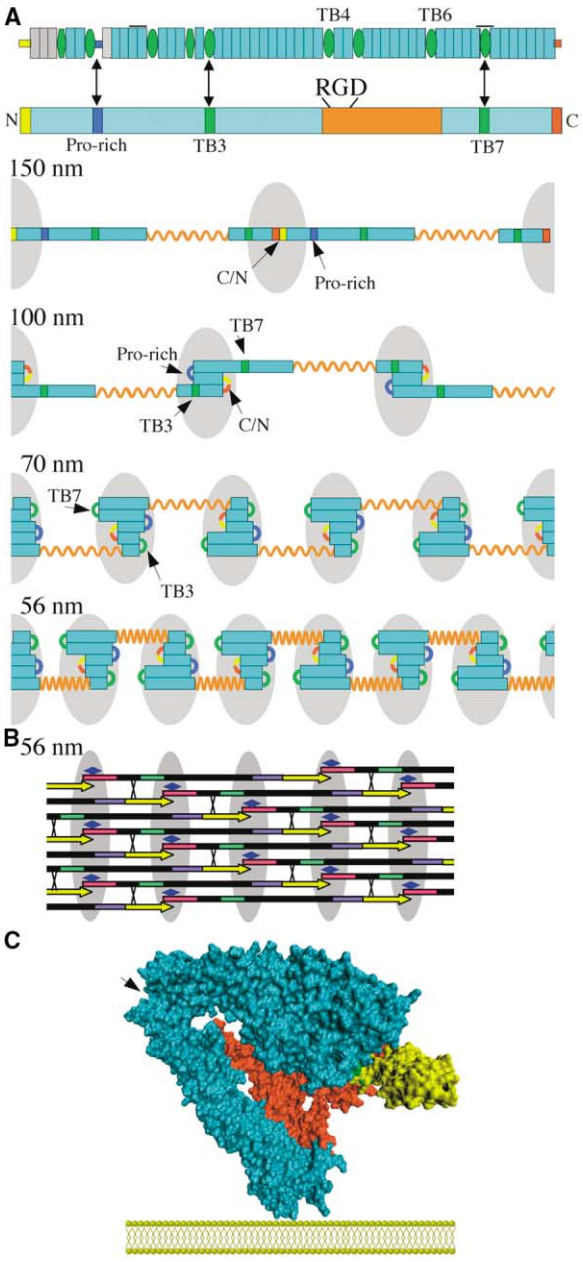

Figure 1. Models of Fibrillin Alignment into Microfibrils and of a Fibrillin-Integrin Complex

(A) A schematic of the progressive folding steps involved in generating the 56 nm bead periodicity (gray ovals) as proposed in the jackknife model (Sherratt et al., 2003) and their predicted location in fibrillin-1 (adapted from Sherratt et al., 2003, with permission). See the text for details. The TB domains are in green, cbEGF in cyan, EGF in gray, proline-rich region in blue, the interbead region in orange, and bead segments in cyan. The N and C termini are in yellow and red, respectively, and transglutaminase crosslink sites overlined.

(B) A second model of the fibrillin microfibril proposed by Lee et al. (see Figure 6A and legend in Lee et al., 2004) leading to the 56 nm periodicity is shown. Arrows, fibrillin-1 molecules; X, intermolecular transglutaminase crosslinks; and diamonds, fibrillin-associated molecules.

(C) Surface representation of a model of an $\alpha V\beta 3$-cbEGF22-TB4-cbEGF23 complex based on docking of the new structure (Lee et al., 2004) on the published crystal structure of RGD-bound $\alpha V\beta 3$ (Xiong et al., 2002). $\alpha V\beta 3$ is a noncovalently associated heterodimer, which assumes a "head" sitting on two "legs" bent at the "knees" (arrow) that are a major site of flexibility in the integrin. The αV subunit is in cyan, $\beta 3$ is in red, and fibrillin in yellow; the green region represents the RGD ligand that binds in the head region, contacting propeller and βA domains of αV and $\beta 3$ subunits, respectively. A schematic of the plasma membrane is shown for orientation. The model was displayed with VMD 1.8.2 software.

raphy and epitope-mapping studies (Figure 1A) suggests that fibrillin molecules initially align into parallel head-to-tail configuration and fold progressively at defined sites between and within successive molecules. Folding at the head-tail junction and a proline-rich region produces an ~100 nm bead periodicity and creates stabilizing transglutaminase crosslinks. Further intramolecular folding at TB-cbEGF linkers results in a 70–80 nm bead periodicity. Elasticity within the interbead segment (comprising TB4-6 and intervening cbEGF domains) allows further compression of the interbead segment into the 56 nm periodicity. Stretching of microfibrils from 56 to 70 nm is reversible, but unfolding above 100 nm appears irreversible, as the bead structure begins to unravel (Baldock et al., 2001). The validity of this model rests on a predicted flexibility of the TB-cbEGF linkages. The recently demonstrated flexibility of the interbead TB6-cbEGF32 linker by NMR (Yuan et al., 2002) supports this prediction.

Fibrillin-rich microfibrils contact cells through integrins, cell surface receptors that mechanically couple the actin cytoskeleton to the ECM (Hynes, 2002). Fibrillin-1 binds integrins $\alpha V\beta 3$ and $\alpha 5\beta 1$ in a divalent-cation-dependent manner through the single RGD motif found in TB4. This interaction induces cell spreading and reorganization of the cytoskeleton and also enhances extracellular fibrillin-1 deposition and the assembly of fibrillins into microfibrils (Bax et al., 2003, and references therein). The nature of the integrin binding interface in fibrillins is unknown.

In the April 2004 issue of *Structure*, Dr. Lee and colleagues report the crystal structure of cbEGF22-TB4-cbEGF23 fragment of human fibrillin that contains the integrin binding RGD motif (Lee et al., 2004). The new crystal structure reveals that the TB4-cbEGF23 linker region is not flexible as previously thought, but is rather incorporated into an extensive largely hydrophobic TB4-cbEGF23 interface. Based on the inflexibility at the TB4-cbEGF23 link, the authors suggest a simpler model of fibrillin packing into microfibrils (Figure 1B), which does not require intramolecular kinks but is still consistent with the available transglutaminase crosslinking and epitope mapping studies. In this "staggered" model, the 56 nm periodicity results from ~12 nm overlap between the N and C termini of successive fibrillin head-to-tail dimers with a one-third staggered alignment. The expected reduced mass density of the beads is compensated for by proteins and proteoglycans known to be present in beads (such as microfibril-associated glycoproteins MAGP-1 and 2 and decorin). Since two TB-cbEGF linkers of roughly equal length exhibit dramatic differences in flexibility, and in view of the variation in linker length and sequence among the other TB-

cbEGF linkers, structural information on the remaining TB-cbEGF pairs (especially the TB3-cbEGF and TB7-cbEGF, predicted to be major folding regions in the jackknife model) will be needed to favor one packing model over the other.

The integrin binding RGD motif in TB4 is located at the tip of a long flexible loop and can be docked onto the cyclic RGD peptide bound to αVβ3 in the αVβ3-RGD crystal structure (Figures 1C and 7A in Lee et al., 2004). This fitting, although imprecise given the high temperature values of the RGD-containing loop in the structure, reveals a spatial proximity of the cb-EGF22 to the ligand binding βA domain of the β3-subunit. When compared to the TB4-cbEGF23 fragment, cb-EGF22-TB4 forms a more stable complex with αVβ3 and elicits more cell spreading and formation of focal contacts. This finding led Lee et al. to suggest that cbEGF22 makes an additional direct contact with βA, engagement of which triggers the observed integrin-mediated signaling events. An alternative explanation however is that cbEGF22 acts indirectly, by stabilizing the integrin binding conformation in TB4. Determination of the structure of a αVβ3-fibrillin complex will be needed to distinguish between these two possibilities.

The RGD motif of fibrillin is located in the interbead segment of assembled microfibrils, which undergoes reversible stretching from 56 to 70 nm periodicity (Sherratt et al., 2003) (Figure 1A). Lee et al. (2004) suggest that this increase in length results from a reversible unraveling of the two β stranded TB4-cbEGF23 linker. This hypothesis needs direct testing. The flexible TB6-cbEGF32 linker, located in the same interbead segment, is likely to contribute more readily to such an extension with yet some contribution from the adjacent TB5-cbEGF25 linker. Binding of TB4 to the integrin, which itself can undergo major flexion/extension movements at its "knees" (Figure 1C) could provide the directionality and support needed to allow recoil.

As is frequently the case, the present structure raises new questions regarding the structural basis of elasticity in fibrillin-rich microfibrils that can now be addressed experimentally. The structure also brings us a step closer to addressing how cells regulate microfibril assembly and elasticity and how this elasticity in turn modulates cell behavior. Answers to these questions have important implications for tissue engineering, wound healing, and diseases of aging.

M. Amin Arnaout
Renal Unit and Structural Biology Program
Massachusetts General Hospital
Harvard Medical School
Boston, Massachusetts 02114

Selected Reading

Baldock, C., Koster, A.J., Ziese, U., Rock, M.J., Sherratt, M.J., Kadler, K.E., Shuttleworth, C.A., and Kielty, C.M. (2001). J. Cell Biol. *152*, 1045–1056.

Bax, D.V., Bernard, S.E., Lomas, A., Morgan, A., Humphries, J., Shuttleworth, C.A., Humphries, M.J., and Kielty, C.M. (2003). J. Biol. Chem. *278*, 34605–34616.

Hynes, R.O. (2002). Cell *110*, 673–687.

Lee, S.S., Knott, V., Jovanovic, J., Harlos, K., Grimes, J.M., Choulier, L., Mardon, H.J., Stuart, D.I., and Handford, P.A. (2004). Structure *12*, 717–729.

Robinson, P.N., and Godfrey, M. (2000). J. Med. Genet. *37*, 9–25.

Sherratt, M.J., Baldock, C., Haston, J.L., Holmes, D.F., Jones, C.J., Shuttleworth, C.A., Wess, T.J., and Kielty, C.M. (2003). J. Mol. Biol. *332*, 183–193.

Xiong, J.P., Stehle, T., Zhang, R., Joachimiak, A., Frech, M., Goodman, S.L., and Arnaout, M.A. (2002). Science *296*, 151–155.

Yuan, X., Werner, J.M., Lack, J., Knott, V., Handford, P.A., Campbell, I.D., and Downing, A.K. (2002). J. Mol. Biol. *316*, 113–125.

Zhang, H., Hu, W., and Ramirez, F. (1995). J. Cell Biol. *129*, 1165–1176.